(12)

Environmental Fluid Mechanics Laboratory
Department of Civil Engineering
Stanford University
Stanford, California 94305-4020

# Multiresolution Feature Analysis and Wavelet Decomposition of Atmospheric Flows

A Final Report on Phase 1 of a Project on the Application of Fractal Concepts to the Analysis of Atmospheric Processes



by

Francis L. Ludwig
James C. Cross III
Robert L. Street

Report EFML 92-1

December 1992



This research was sponsored by
The Marine Meteorology Program
Ocean Sciences Division
Office of Naval Research
Grant N00014-89-J-1794

## Abstract

This is the final technical report on ONR Grant N00014-89-J-1794, entitled "Application of Fractal Concepts to the Analysis of Atmospheric Processes", for the period from 1 April 1989 through 30 September 1991. The goal of the research was to improve understanding of atmospheric processes through the application of analytical approaches derived from methods that have been associated with fractal and wavelet methods. This was the first phase of ongoing work that is now supported by a new grant for the period to 30 September 1994.

There were two major thrusts of this work to date. First, we have applied multiresolution feature analysis to an atmospheric data set. In the process the analysis was extended to three-dimensional vector fields. To make the three-dimensional vector features "imaginable," we have adopted the a variant of the Lorenz concept of empirical orthogonal functions or EOF. These allow representation of empirically-defined patterns of small-scale atmospheric motions. Second, we developed a strategy for the generalized wavelet analysis of homogeneous turbulence. The strategy calls for decomposition of a collection of direct numerical simulation data sets for homogeneous turbulence in a stratified Boussinesq fluid subject to an imposed shear, in both two and three dimensions.

## Table of Contents

## 1. Introduction

This final technical report for Grant N00014-89-J-1794, entitled "Application of Fractal Concepts to the Analysis of Atmospheric Processes", covers the period from 1 April 1989 through 30 September 1991. The project began as one focused on fractal methods, but it was expanded during the course of the work. The work described herein represents the initial phases of the project and its status through the end of the above grant; a new grant was awarded to continue the work until September 1994.

The goal of the research is to improve our understanding of atmospheric processes through the application of analytical approaches derived from methods that have been associated with fractal and wavelet analyses. We seek, first, a clear understanding of the spatial and temporal characteristics of atmospheric motions that contain many scales and are intermittent; second, we seek to determine the causes of key features of these motions.

Our near term objectives included:

Thrust 1: Multiresolution Feature Analysis: To identify and obtain existing data that are suitable for studying spatial distributions of atmospheric properties [including aerosols and plume materials], to develop analysis methods and the computer algorithms and codes necessary to apply them, to apply the analysis methods to atmospheric observations, to interpret the results of the analyses to identify and characterize important physical processes, and to communicate the results of the analyses and interpretations.

Thrust 2: Wavelet Analyses: To identify and/or create appropriate wavelets for application in the analysis of field data and direct numerical simulations of atmospheric-type flows. A key question to be answered [which has not been rigorously answered yet] is "Given a signal or data sample, what analyzing wavelet ought to be used to examine it?" We seek a criterion or criteria of optimality driven by the objectives of the analysis, i.e., what do we seek to learn?

Appendixes 1 and 2 contain, respectively, a publication and a list of presentations on the work supported by the grant. Appendix 3 contains a few relevant references.

## 2. Multiresolution Feature Analysis

The multiresolution feature analysis [MFA] methodology developed by Jones, et al. (1988) was programmed and applied to lidar and transmissometer smoke plume imagery. Other fractal dimension calculation methods are also being programmed and used on these data. The MFA method successively degrades image resolution by half, applies a "feature-detecting filter" to the degraded images, and examines the changes in the number of features whose "intensity" exceeds different thresholds. The statistical relationships among features at different scales define scaling parameters and fractal dimensions.

We extended the MFA concepts so that they can be applied to atmospheric vector fields. In essence, the usual scalar filtering techniques have been redefined to replace the arithmetic products of numbers with inner (dot) products between vectors. We had intended to define features that have some special physical significance, but had difficulty specifying more than a very few, so we sought an objective method for defining 'physically significant features."

Lorenz (1956) used a variant of principal component analysis to define empirical orthogonal functions (EOF) that represented different patterns of variability in atmospheric

pressure fields over the U. S. Ludwig and Byrd (1980) adapted this technique to identify vector patterns that accounted for the most variance in a data set. The use of these techniques for defining those small scale patterns of variability that explain most of the variance seemed a logical approach to the definition of features to be used with the MRF analysis. The program necessary to calculate the most important EOFs for small sections of three dimensional vector fields has been written and applied to Schneider's wind data [see Appendix 1]. A corresponding methodology for scalar fields has been programmed and is being tested. Available lidar and transmissometer smoke plume observation data appear to have artifacts that lead to anomalous results.

The first task of this study was to identify and acquire suitable data for analysis. This task has largely been completed. However, this is the kind of task that never completely ends and we will continue trying to identify suitable data for analysis. In fact, we recently identified a large eddy simulation (Costigan, 1992) of the same situation described by Schneider's wind data. These results are being obtained. The data acquired include large eddy and direct numerical simulation results, dual Doppler radar observations of atmospheric motions, lidar cross sections and transmissometer imagery through smoke plumes, and a digitized weather satellite image of marine clouds.

Much of the second task which was to identify analysis approaches has been done, but we continue to identify potentially useful approaches that deserve to be pursued. Computer programs have been written for calculating the fractal dimension of two dimensional scalar fields by box counting, Fourier filtering and multiresolution feature analysis methods. The programs have also been written for identifying physically significant features for the MFA methodology. Some of these programs have been applied to various data sets in accordance with the third task, but little of the interpretation task has been done.

The primary product of this thrust area to date is the paper displayed in Appendix 1.

## 3. Wavelet Analyses

To analyze scale interactions in a fluid dynamical field one would like to have the ability to consider space and time and their respective scales simultaneously. This suggests using a multiresolution analysis based on the wavelet transform, an operation originally defined in a paper by Grossman and Morlet (1984). Our initial approach was direct, namely, to study the known and successful wavelets, e.g., Morlet, Mexican-hat, etc., and to ascertain their properties in a systematic way, with particular focus on what the wavelet-transformed data signal tells us. In a majority of the published reports, wavelets have been applied in an ad hoc fashion, with little commentary regarding the preference of one wavelet over another. Our experiments with a number of wavelets indicated that the choice of wavelet is fairly inconsequential. Accordingly, for our ongoing work, we have opted to use a class of scale-based filters which are very nearly true wavelets, namely Fourier bandpass (FBP) filters. In physical space these filters are the difference of two appropriately scaled *sinc* functions of different amplitudes and widths.

Our strategy calls for the use of wavelets to offer new insights in regard to the dynamics of stratified flows. The data for this analysis will be a collection of direct numerical simulation data sets. We will consider homogeneous turbulence in a stratified Boussinesq fluid subject to an imposed shear, in both two and three dimensions. This is a generalization which includes isotropic decay, decay of turbulence in a stratified fluid, and shear of a uniform density fluid as special cases. This scenario covers most cases of practical interest, especially in the context of smaller scale geophysical flows. We envision the application of the wavelet methodology to the following: (1) classification of flow

structure, (2) mixing efficiency measures, and (3) internal wave / turbulence discrimination.

Appendix 1. *"Subkilometer Spatial Variability of Winds in a Sheared, Convective Atmospheric Boundary Layer"* by Ludwig, Schneider and Street

Reprinted from the preprint volume of the Tenth Symposium on Turbulence and Diffusion, 29 Sept. - 2 Oct. 1992, Portland, OR. Published by the American Meteorological Society, Boston, MA

7.3

# SUBKILOMETER SPATIAL VARIABILTY OF WINDS IN A SHEARED, CONVECTIVE ATMOSPHERIC BOUNDARY LAYER

by F. L. Ludwig*, J. M. Schneider** and R. L. Street*

## 1. INTRODUCTION

This work evolved from an effort to use fractal concepts to interpret atmospheric behavior into one where some of the techniques used to calculate fractal dimension have been used to study the nature of the air motions themselves, providing new insights into Richardson's (1922) little verse:

"Big whorls have little whorls,
Which feed on their velocity;
And little whorls have lesser whorls,
And so on to viscosity . . . "

We have attempted to define Richardson's whorls. This would not have been possible without the dual Doppler radar wind data from the 1984 Phoenix II project.‡

## 2. DUAL DOPPLER RADAR WIND DATA

The Phoenix II data have unusual three-dimensional resolution on a grid with 200 m spacing between points (in all three directions) over a 9×9 km area to a depth of 2 to 3 km. Temporal resolution was about two minutes. Three-dimensional wind vectors (vertical components were inferred from continuity assumptions) are available. Some data are missing because the radar volumes did not overlap at the corners, or there was often insufficient chaff at the upper levels, but the spatial resolution is still sufficient that we were able to develop the analytical approaches discussed later.

The observation area (about 20 km east of the foothills of the Rocky Mountain Front Range and about 50 km east of a reasonably uniform ridge of the continental divide) is relatively flat, with undulations of about ±50 m around an average elevation of 1600 m ASL. The relative proximity to the mountains appears to have controlled the flow. Weak easterly surface winds (~3 m $s^{-1}$) and the strong isolation suggested a typical convective planetary boundary layer (PBL), well-mixed and capped by a strong inversion. Aircraft and radar data indicated otherwise. Each of the days (17 and 22 June 1984) chosen for analysis had a multi-layered structure. The locally generated convective layer was interacting with an over-running, slightly stable layer of moderate turbulence that had probably formed as a convective PBL over the mountains. The westerlies that advected this over-running layer, combined with the underlying easterlies to maintain a strong shear throughout the depth of the PBL. This shear persisted in spite of the afternoon convection which suggests a thermally driven easterly flow in the lower layers, induced by the warm, east-facing mountain slopes. The strong persistent shear induced important vertical motions. The turbulent kinetic energy budget for these flows (Schneider, 1991) shows shear generation that was frequently as great, or greater than buoyant production above the lowest kilometer. There were more than the usual thermals ascending until their buoyancy is lost to entrainment, or they are stopped by an inversion layer aloft. Buoyant forcing *and* shear-generated eddies determined vertical motion.

The most unstable of the periods analyzed (22 June 1984, 12:40–13:00 Mountain Standard Time) had a rich mix of vorticity structures (Schneider, 1991) that evolved and interacted throughout the period. The largest and longest-lived of the vortex filaments were near the level where the mean winds changed from easterly to westerly. They were kilometers long and persisted for more than ten minutes, with an orientation that was roughly horizontal and normal to the shear, i.e. approximately north-south. Shorter (in both length and duration) vorticity features parallel to the shear, at altitudes above and below the major features also appeared.

There were more stable cases too, when the convection was much less vigorous. These boundary layers were decaying because of subsidence, or decreased surface heat flux. In one (17 June 1984, 15:00–15:21 MST), there was very little vertical motion or turbulent kinetic energy production. That case provides an interesting contrast with the unstable case just described. We focus on these two, very different cases.

Schneider (1991) has described the processing of the original data in detail. Each volume scan provided information from about $10^5$ volumes, each about $2.7\times10^6$ $m^3$ (~140 m on a side). The processing to obtain winds in Cartesian coordinates inherently smoothed the measurements. Cressman weighted averaging was used to get the two radial wind components (one from each radar) on a Cartesian grid; it provides a nearly uniform filtering that is consistent with the volume averaging introduced by the radar observations. Additional Leise (1981) filtering was used for numerical smoothness. Radial winds were linearly interpolated between successive observations to common times. A standard package of NCAR programs (CEDRIC; Mohr et al., 1986) was used to calculate u, v, and w components from the radar observations and the continuity equation.

## 3. MULTIRESOLUTION FEATURE ANALYSIS

### 3.1 Scalar Fields

Jones et al. (1991) define multiresolution feature analysis (MFA) to have the following steps:

1. Repeatedly smooth and resample a scalar field, giving a new field at each step with half the resolution.
2. Apply a feature detector to the fields from step 1.
3. Identify peaks in the fields produced in step 2.
4. Count the peaks from step 3 that exceed each of a range of threshold values for each resolution.
5. Rescale and plot the results -- $(S_i)^2(n_y)_i$ versus $y/(S_i)^k$.

where $S_i$ is the $i^{th}$ spatial scale; $(n_y)_i$ is the number of peaks exceeding the threshold y at the $i^{th}$ resolution. A scaling field

* Environmental Fluid Mechanics Laboratory, Stanford University, Stanford, CA 94305.

** Cooperative Institute for Mesoscale Meteorological Studies, University of Oklahoma, Norman, OK 73019

‡ Supported by the National Center for Atmospheric Research (NCAR), the Army Research Office (ARO), and the Wave Propagation Laboratory (WPL) of the National Atmospheric and Oceanic Administration's Environmental Research Laboratories.

has a value of k that produces a set of invariant relationships; k is related to the fractal properties of the distribution of the features. Our interest here is in the smoothing, and the definition and application of feature detectors, the first two steps in the above list.

The smoothed value at a point is obtained from a weighted average of values at surrounding points. The smoothed field will have one-quarter as many points, each representing four times the area of a cell in the original, higher resolution field. The smoothing eliminates smaller scale features. Feature detection as described by Jones et al. (1991) works in much the same way as the smoothing, except that the value at a point is given by the sum of the products of the surrounding values with a template of numbers representing the feature to be detected. For example a detector for a vertically oriented "edge" might consist of a 3x3 array of numbers, with the first column made up of positive values, the middle of zeroes and the third of negative values. When this template is placed over a region of strong gradient from left to right, it will produce a large positive value. Other configurations can be devised to respond to other specific patterns.

### 3.2 Extension to Three-Dimensional Vector Fields

Smoothing is much the same in either two or three dimensions, differing for the latter only in that the filter will be three-dimensional. The definition of vector "features" is somewhat subtler. Either one can apply the technique to some scalar property of the vector field (e.g. divergence or vertical vorticity component ), or define vector features and apply the multiresolution methodology directly, i.e. the definition of features as three-dimensional arrays of vectors over small subregions. The latter approach was taken. The vector feature detectors are defined so that their output is the sum of the scalar products of their component vectors with the corresponding vectors in the field being analyzed. The result is a three dimensional array of scalar "feature intensities." One of the important differences between this approach and conversion to scalars before the feature analysis, is that the results can be interpreted as specific kinds of "whorls."

### 3.3 Empirical Definition of Vector Features

It has been difficult to imagine three-dimensional vector features, so we devised a method by which the data would determine important patterns of small scale variability. Our approach goes by many names (e.g. principal component, eigenvector, or factor analysis). It represents the data in terms of a set of linearly independent basis functions, which Lorenz (1956) called empirical orthogonal functions -- EOF. This abbreviation is generally understood, and can be reinterpreted to mean empirical orthogonal *features*, a more apt description for this application.

EOF features are: (1) based on the characteristics of the data themselves, (2) linearly independent of one another, and (3) characterized by a measure of their relative importance. Past EOF applications have focussed on scalar features or sets of basis functions for numerical calculations. Lorenz' (1956) patterns of atmospheric pressure at 64 stations in the United States was a scalar application. Lumley (1967, 1980) suggested similar analyses to extract coherent structures from turbulent flows. He used complex number representation of vectors over the entire domain. Others (Hardy, 1977; Ludwig and Byrd, 1980) used vector EOFs to classify inputs for wind models. Sirovich (1988) analyzed numerical simulations with EOFs.

Lorenz (1956) provides a complete discussion of the use of EOFs for representing maximum variance (i.e., information) in a data set with fewer descriptors. Parameter values representing the state of some system can be represented by:

$$\begin{bmatrix} P_1-\overline{P}_1 \\ P_2-\overline{P}_2 \\ \vdots \\ P_M-\overline{P}_M \end{bmatrix} = q_1(t)\begin{bmatrix} y_{11} \\ y_{21} \\ \vdots \\ y_{M1} \end{bmatrix} + q_2(t)\begin{bmatrix} y_{12} \\ y_{22} \\ \vdots \\ y_{M2} \end{bmatrix} \cdots + q_M(t)\begin{bmatrix} y_{1M} \\ y_{2M} \\ \vdots \\ y_{MM} \end{bmatrix} \tag{1}$$

The left hand side (LHS) is the set of observed parameters minus their individual mean values over all cases. The q's are specific to each subregion, and can be used to replace the original descriptors. If all the q's are used, the observations are represented exactly. If the sequence is truncated, the representation is approximate. The y vectors are the EOFs, arranged in decreasing order of explained variance. They can be interpreted as patterns of variability about the mean. The coefficients $q_k$ are the inner (scalar) products of the observation column vector (LHS of Eq. 1) with the corresponding unit EOF vector (the y's on the RHS). The y's are the eigenvectors of the covariance matrix $(\mathbf{P}\text{-}\overline{\mathbf{P}})\ (\mathbf{P}\text{-}\overline{\mathbf{P}})^T$ formed by multiplying the data (relative to their means) matrix by its transpose. The eigenvector calculation is straightforward with available FORTRAN subroutines such as are provided in Numerical Recipes (Press et al., 1987).

The approach here differs from others in that it uses small 3x3x3 subsections of the observed wind field. The middle vector is subtracted from each of the surrounding 26 vectors to obtain a difference vector ($\Delta$V) at each point in the subsection:

$$(\Delta V_{ijk})_m = \begin{bmatrix} \Delta u_{ijk} \\ \Delta v_{ijk} \\ \Delta w_{ijk} \end{bmatrix}_m = \begin{bmatrix} u_{ijk}-u_{222} \\ v_{ijk}-v_{222} \\ w_{ijk}-w_{222} \end{bmatrix}_m , \tag{2}$$

where $u_{ijk}$, $v_{ijk}$ and $w_{ijk}$ are vector components at point ijk in the $m^{th}$ subsection; 222 is the center point. The 3-dimensional array of $\Delta$Vs shows the local pattern of motion. If we have this array and the vector $V_{222}$ at the center point, the surrounding 26 vectors can be reconstructed. The deviations $\Delta V'$ about the averages (for the same relative points in all the N subsections) are described by [(3x3x3) −1] grid points x3 vector components, i.e. 78 components for each column vector describe the *state* of a small subcube. The matrix of these *state vectors* is multiplied by its transpose to give the covariance matrix from which the EOFs are found. Those EOFs that explain the most variance in the individual patterns can be used as the *features* in the modified multiresolution feature analysis methodology. They can also be considered in some sense to represent Richardson's whorls.

Data from several times during a seqt ence (generally spanning ~20 minutes) were combined so that more than 150,000 3×3×3 subvolumes were typically available for analysis. The data matrix was formed from a randomly selected sample of ~10 percent of the total to reduce computation and memory requirements. We repeated the process for ten different samples from each of 7 data blocks to check the variability of the results one random sample to another. Fewer than 10% of the averages differed by more than 1%. Inner products were used to compare the ten EOFs that explained the most variance for a particular random sample with those based on other random samples from the same data set. More than half the corresponding inner products exceeded 0.98. A value of 1 indicates perfect agreement.

## 4. EXAMPLES OF EMPIRICALLY DEFINED PATTERNS OF SMALL-SCALE ATMOSPHERIC MOTION

### 4.1 Averages

Figures 1 and 2 show average patterns of small- and medium-scale variability for stable and unstable examples, respectively. The vector at the center serves as a scale, pointing northeast at 1 $ms^{-1}$. The solid arrows indicate the horizontal wind, while the gray arrows show vertical motion. Both stable and unstable cases show the average shear that was mentioned earlier. It is stronger in the stable case. The apparent greater shear for 400 meter resolution is because the separation between the planes is twice that for the 200 m resolution.

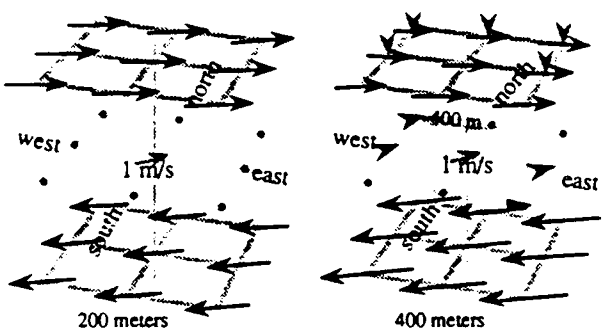


Fig. 1. Averages for two resolutions -- stable case

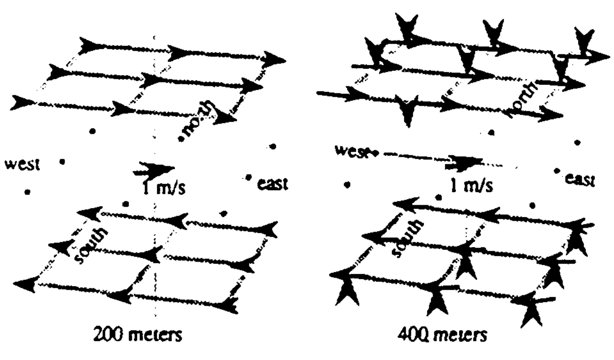


Fig. 2. Averages for two resolutions -- unstable case

### 4.2 Empirically Defined Features

The 200 m resolution EOFs for stable and unstable cases differ appreciably, both in their nature and in the amount of variance they explain. The first two stable case EOFs (Figure 3) explain 37% and 21% of the variance, while the unstable case EOFs (Figure 4) explain 17% and 12%, supporting the intuitive notion that an unstable, turbulent atmosphere displays a much wider variety of motions than a stable one. Figure 3 shows the dominant variability pattern (EOF 1) to be a local change in the shear. The stable case EOF 2 also changes the shear locally, but in the opposite sense in the lower and upper halves. Neither feature introduces a major change in vertical motion. Similar patterns were found in other stable cases. In one instance EOF 1 explained nearly half the total variance.

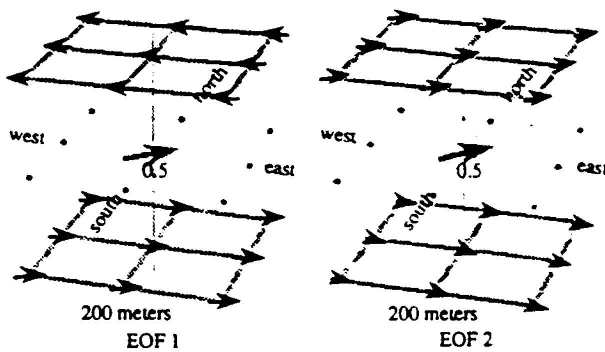


Fig. 3. 200 m resolution EOF 1 and EOF 2 -- stable case

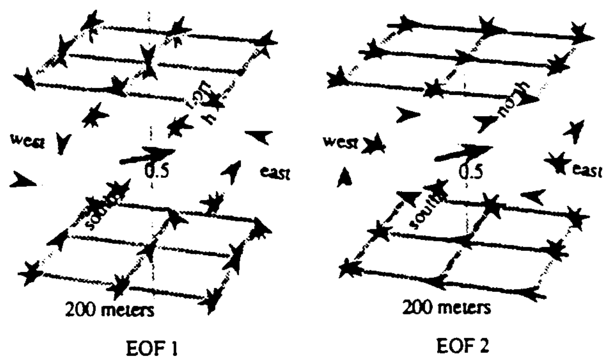


Fig. 4. 200 m resolution EOF 1 and EOF 2 -- unstable case

The EOFs for the unstable case are characterized by more vertical motion than for the stable. This is not surprising for a more convectively active atmosphere. They also show more evidence of rotation. EOF 1 appears to be a section of a vortex tilted about 45° from the vertical, pointing in the direction of the shear. The vertical vorticity component would be increased when the sense of this feature is positive and decreased for negative coefficients. The vertical motion is upward to the northwest and downward toward the southeast for a positive feature value. EOF 2 tends to enhance the overall shear when positive. It also introduces vertical motions, upward to the southwest and downward to the northeast.

The EOFs determined from the 400 m resolution smoothed data are shown in Figures 5 and 6. Again, the stable case EOFs explain more variance -- 40% and 12% for the stable case, versus 17% and 14% for the unstable case. EOF 1 for the stable case enhances the shear for the 400 m resolution data, but mostly in the lower half of the feature. This reflects the nonuniformity of shear, a tendency to decrease with height. This EOF also has a small component of subsidence at several points, suggesting shear enhancement in subsiding air. Values of the 400 m resolution, stable EOF 2 greater than zero introduce subsidence at the upper and lower levels, enhanced westerlies aloft, and increased southerly components below.

The 400 m resolution EOF 1 for the unstable example (Figure 6) is similar to that for the 200 m resolution, although the tilt of the vortex is not as pronounced. EOF 2 for the coarser resolution has little effect on the horizontal components. Instead, it tends to introduce subsidence (for positive values) throughout its volume.

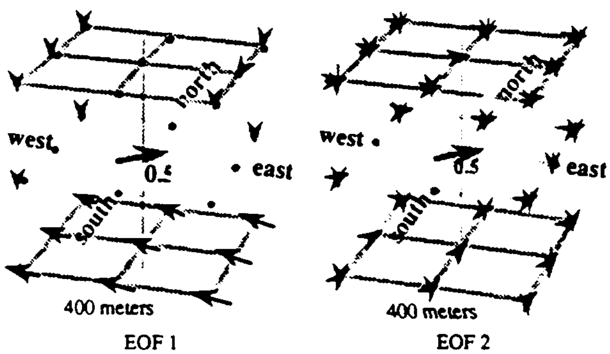


Fig. 5. 400 m resolution EOF 1 and EOF 2 -- stable case

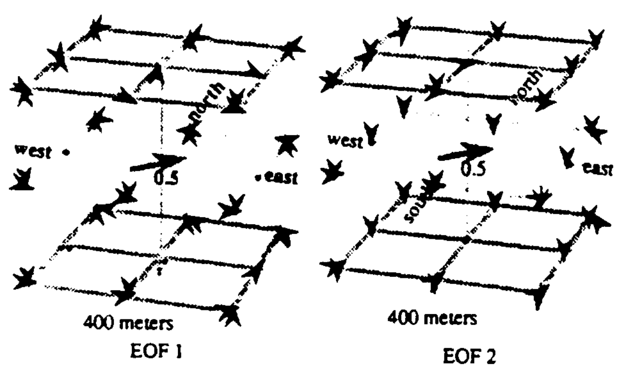


Fig. 6. 400 m resolution EOF 1 and EOF 2 -- unstable case

## 5. CONCLUSIONS

The wind analysis technique discussed here has provided some interesting information about the small scale variability of atmospheric motions. The technique has considerable potential that we have not yet exploited. We have only begun to examine the spatial relationships between the intensities of features at different resolutions. One can imagine that the feature intensities associated with modeled vectors on a coarse array could serve as a basis for estimating a distribution of smaller features, thereby permitting the estimation of a field with finer resolution. We expect to continue the multiresolution feature analysis and examine the fractal properties of the flow. It will be particularly interesting to see if different features exhibit different scaling properties.

Acknowledgements: We gratefully acknowledge the support of the Office of Naval Research (through Stanford University), the Army Research Office (through SRI International and the Cooperative Institute for Mesoscale Meteorological Studies), and the National Science Foundation and the National Oceanic and Atmospheric Administration (through CIMMS). We also wish to thank the NOAA Wave Propagation Laboratory for the original Doppler wind measurements.

## REFERENCES


Hardy, D. M., 1977: "Empirical Eigenvector Analysis of Vector Observations," *Geophys. Res. Letters, 4,* 319-320.

Jones, J. G., R. W. Thomas, and P. G. Earwicker, 1988: Multi-Resolution Analysis of Remotely-Sensed Data, *Int. J. Remote Sensing, 12,* 107-124.

Leise, J. A., 1981: "A multidimensional Scale-telescoped Filter and Data Extension Package," National Oceanic and Atmospheric Administration Technical Memo. ERL/WPL-82, Wave Propagation Lab., Boulder, CO, 20 pp.

Lorenz, E. N., 1956: "Empirical Orthogonal Functions and Statistical Weather Prediction," Scientific Report 1, Statistical Forecasting Project, Mass. Inst. Tech., Cambridge, Mass. (Def. Doc. Ctr. No. 110268), 49 pp.

Ludwig, F. L. and G. Byrd, 1980: "A Very Efficient Method for Deriving Mass Consistent Flow Fields from Wind Observations in Rough Terrain," *Atmos. Environ, 14,* 585-587.

Lumley, J. L., 1967: "Coherent Structure in Turbulence," *Atmospheric Turbulence and Radio Wave Propagation,* (A. M. Yaglom and dV I. Tatarski, editors), Nauka, Moscow, 166-178. (Cited by Sirovich, 1988).

Lumley, J. L., 1981: "Coherent Structures in Turbulence," *Transition and Turbulence* (R. E. Meyer, ed.), Academic Press, New York, 215-242.

Mandelbrot, B. B., 1983: *The Fractal Geometry of Nature,* W. H. Freeman and Co., NY, 468 pp.

Press, W. H., B. P. Flannery, S. A. Teukolsky and W. T. Vetterling, 1986: *Numerical Recipes,* Cambridge University Press, Cambridge, 818 pp.

Richardson, L.F., 1922: *Weather Prediction by Numerical Process,* Cambridge University Press. (Cited by Mandelbrot, 1983)

Schneider, J. M., 1991: *Dual Doppler Measurement of a Sheared Convective Boundary Layer,* Ph D Dissertation, Univ. of Oklahoma, Norman, Oklahoma, 134 pp.

Sirovich, L., 1988: "Analysis Turbulent Flows by Means of Empirical Eigenfunctions," Center for Fluid Mechanics Report No. 90-212, Brown Univ., Providence, RI, 40 pp.

## Appendix 2. Presentations


Ludwig, F. L. 1991a, "Using Multi-resolution Feature Analysis to Interpret Atmospheric Observations," *Proc. 11th EOSAEL / TWI Conf.*, U. S. Army Atmos. Sci. Lab., White Sands Missile Range, NM, 623-631.

Ludwig, F. L. 1991b, "Multi-Resolution Feature Analysis of Atmospheric Motion Using Empirically Defined Features," *Dynamic Days Workshop*, Berlin.

Ludwig, F. L. 1991c, "Empirically Defined Structures in a Sheared Convective Boundary Layer," *Fall 1991 Meeting of the American Geophysical Union*, San Francisco.

## Appendix 3. References


Costigan, K. R. (1992), "Large eddy simulation of the atmospheric boundary layer East of the Colorado Rockies," Colorado State University, Department of Atmospheric Sciences, Paper No. 511, 142 pages.

Grossman, A., and Morlet, J. (1984), "Decomposition of Hardy functions into square-integrable wavelets of constant shape," *SIAM J. Math. Anal., 15, 4*, July.

Jones, J. G., Thomas, R. W., and Earwicker, P. G. (1988), "Multi-resolution analysis of remotely-sensed data," *Int. J. Remote Sensing, 12,* 107-124.

Lorenz, J. A. (1956), "Empirical orthogonal functions and statistical weather prediction," *Scientific Report 1, Statistical Forecasting Project,* Mass. Inst. Tech., (Def. Doc. Ctr. No. 110268), 49 pages.

Ludwig, F. L., and Byrd, G. (1980), "A very efficient method for deriving mass consistent flow fields from wind observations in rough terrain," *Atmos. Environ., 14,* 585-587.